

Parametric and Machine Learning-Based Analysis of the Seismic Vulnerability of Adobe Historical Buildings Damaged After the September 2017 Mexico Earthquakes

Rafael Ramírez Eudave ^a, Tiago Miguel Ferreira ^b, Romeu Vicente ^c, Paulo B. Lourenco ^a,
and Fernando Peña ^d

^aInstitute for Sustainability and Innovation in Structural Engineering (ISISE), Department of Civil Engineering, University of Minho, Guimaraes, Portugal; ^bSchool of Engineering, College of Arts, Technology and Environment (CATE), University of the West of England (UWE Bristol), Bristol, UK; ^cRISCO, Departamento de Engenharia Civil, Universidade de Aveiro, Aveiro, Portugal; ^dInstituto de Ingeniería, Universidad Nacional Autónoma de México, Mexico City, Mexico

ABSTRACT

In September 2017, two strong earthquakes hit the central region of Mexico, producing substantial damage to the historical buildings. A retroactive analysis for assessing the pre-event seismic vulnerability of these constructions allowed for testing the suitability of an existing parameter-based approach based on material and geometrical features. More than 160 adobe buildings in four municipalities of the State of Morelos were surveyed and included in a vulnerability-oriented GIS database. Data were collected on-site and managed by resorting to open-source GIS software combined with a Python-based database management tool and a cloud-based platform for onsite data collection using mobile devices. The parameter-based approach was used for assessing the analytical seismic vulnerability of the buildings and implementing a secondary, more conservative assessment that considers uncertainties associated with the data acquisition process. The capabilities of the database were further used to train a Machine Learning algorithm aimed at overcoming some representativeness limitations of the parameter-based analytical method. This third approach was found to be suitable for assessing the vulnerability of the building typologies addressed in this investigation. Although the implementation discussed in this paper is limited to a specific vernacular typology, it can be used to conduct customized local calibrations.

ARTICLE HISTORY

Received 18 December 2022
Accepted 3 April 2023

KEYWORDS



Geographical Information System; adobe; damage database; field survey; machine learning; seismic damages; seismic vulnerability assessment

1. Introduction

According to the United Nations International Strategy for Disaster Reduction (United Nations International Strategy for Disaster Risk Reduction 2009), vulnerability is defined as “the characteristics and circumstances of a community, system, or asset that make it susceptible to the damaging effects of a hazard”. Assessing the seismic vulnerability of the existing building stock is critical to the definition and implementation of proactive and reactive seismic risk mitigation actions (Ferreira, Maio, and Vicente 2017; Salazar and Ferreira 2020). Nevertheless, the evaluation of large numbers of buildings poses numerous challenges related to the heterogeneity among existing constructions. This aspect is more explicit when dealing with historical buildings, typically subjected to many sources of uncertainty. Some common analytical strategies may be unsuitable for performing fast and reliable structural analysis at the urban scale (e.g., structural

analysis based on numerical models), bringing attention to more empirical approaches based on the identification of characteristics that seem to enhance the seismic performance of structures.

A relevant precedent of this approach for Reinforced Concrete buildings has been developed by (Ruggieri et al. 2022), combining a typological classification of structures with a series of standard numerical models for building fragility curves. In this case, the data extraction is aided by Machine Learning algorithms, which label each building according to a series of externally recognizable features. This tool, known in the literature as Vulnerability Analysis using Machine Learning (VULMA) (Ruggieri et al. 2021), is composed of a series of modules that recognize typological patterns from raw data, including pictures. This process is possible given expert judgement-based training in which a series of categories are manually assigned. Although the need for fulfilling some typological assumptions constrains

CONTACT Tiago Miguel Ferreira  Tiago.Ferreira@uwe.ac.uk  School of Engineering, College of Arts, Technology and Environment (CATE), University of the West of England (UWE Bristol), Bristol, UK

© 2023 The Author(s). Published with license by Taylor & Francis Group, LLC.

This is an Open Access article distributed under the terms of the Creative Commons Attribution License (<http://creativecommons.org/licenses/by/4.0/>), which permits unrestricted use, distribution, and reproduction in any medium, provided the original work is properly cited. The terms on which this article has been published allow the posting of the Accepted Manuscript in a repository by the author(s) or with their consent.

the application of this approach, it was found suitable for assessing large sets of constructions.

In the case of unreinforced masonry constructions, the approach developed by (Rosti, Rota, and Penna 2021) builds up on a preliminary categorization based on the classifications created after the Irpinia (1980) and L’Aquila (2009) earthquakes for building statistical distributions to get a set of relevant typological features that are then compared against the observed levels of damage. By following this approach, the authors have derived a set of empirical fragility curves representative of the seismic vulnerability of typologically compatible buildings.

This knowledge, based on long-term observations of failure and success, has determined constructive traditions and vernacular architecture principles worldwide. It is worth noting that the development of these empirical processes is not substantially different to the training of computational algorithms, in which a series of existing incomes and outcomes are analysed to find patterns and relations for predicting the outcome of new income data.

1.1. The earthquakes of September 2017 in Mexico

On the 7th of September 2017, an earthquake ($M_W = 8.2$) hit the south coast of Mexico. This event, later known as

the Tehuantepec Earthquake, had its origin 133 km southwest of Pijijiapan (State of Chiapas).

There was extensive damage in the building stock, namely in adobe and unreinforced masonry structures in the states of Oaxaca and Chiapas (Godínez et al. 2019). On the 19th of September 2017, the so-called Puebla-Morelos Earthquake ($M_W = 7.1$) hit the south centre of the country (Figure 1).

This event had its epicentre 12 km southeast Axochiapan (State of Morelos), ca. 120 km away from Mexico City, producing the collapse of at least 46 structures in the capital (Alberto et al. 2018; Buendía and Reinoso 2019). Both events left behind a large number of houses with medium and severe damage in the central and southern regions of the country (see Table 1).

1.2. Impact and loss of historical buildings

According to the Global Assessment Report of Disaster Risk Reduction Atlas (United Nations Office for Disaster Risk Reduction 2017), seismic events in Mexico are responsible for annual average losses ranging between 1,001 and 2,000 million USD. The figures for the 2017 events are even more significant, with estimated reparations costs reaching between 2,000

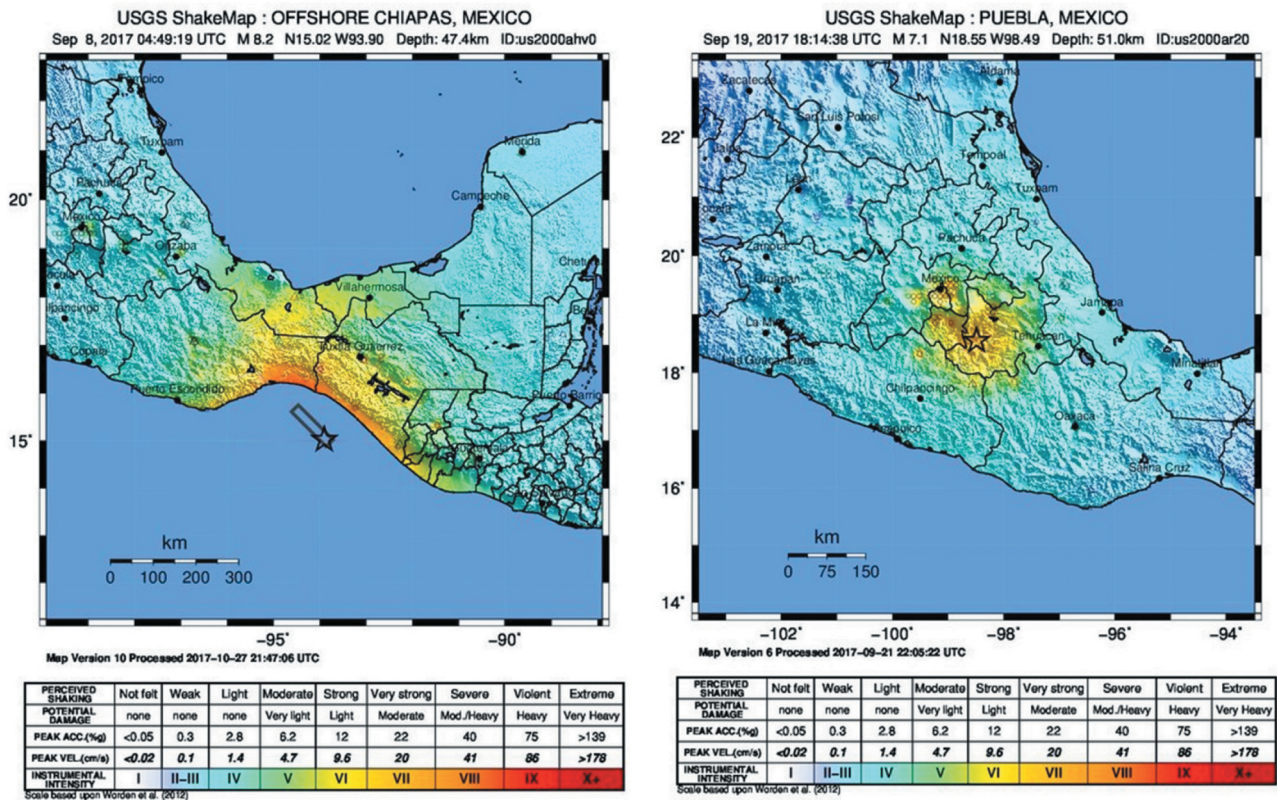


Figure 1. USGS Shake maps for the Pijijiapan (left) and Puebla-Morelos (right) Earthquakes (Geodetic Facility for the Advancement of Geoscience 2023).

Table 1. Affected housing units per State as a result of the Earthquakes of the 7th and 19th of September, 2017 (de la Republica 2017).

State	Housing units	
	Damaged	Collapsed
State of Mexico	6,059	2,468
Mexico City	5,765	2,273
Morelos	15,352	1,323
Puebla	27,812	3,214
Oaxaca	63,336	21,823
Chiapas	59,397	18,058
Guerrero	2,976	1,451

and 4,500 million USD due to ca. 180,000 affected houses (ca. of 0.56% of the total of housing units registered in the national census). States like Oaxaca (6.07%), Chiapas (4.71%), and Puebla (1.79%) have been particularly affected, with around 6%, 5%, and 2% of their buildings stocks, respectively, heavily affected by the quake (Caprano, Ortiz, and Valencia 2018; Ramírez Eudave, Ferreira, and Vicente 2022). The Mexican Civil Protection authority (de la Republica 2017) estimated 369 human losses and 180,731 damaged houses (from which a 28% was reported as total loss).

In the context of cultural architectonic heritage, the Mexican Secretary of Culture estimated that some 2340 historical monuments were affected, including 1,680 temples built before 1900 (Ramírez Eudave and Ferreira 2021). Nevertheless, the number of damaged historical housing units is still unknown. These ancient houses are particularly significant in the states of Morelos and Puebla (commonly built in adobe), in which damages were proportionally more extensive (Galvis et al. 2017). Adobe structures in Morelos represent ca. 4.5% of housing units (Sánchez Calvillo, Alonso Guzmán, and López Núñez 2021), reaching proportions of more than 20% in other municipalities (undefined). The development of a vernacular tradition of adobe structures in this region is closely linked to the occurrence of seismic events, shaping specific and adapted building typologies (Guerrero Baca 2019). The scale of damages in several settlements after the Puebla-Morelos earthquake urged immediate intervention due to the humanitarian crisis derived from the collapses and the lack of services, being declared as disaster zones (Ortiz et al. 2018).

A relatively common reaction to the loss or damage of adobe-based buildings was their replacement with new houses by using more industrialized building systems and technology, including prefabricated modules. This process is the product of one or several of the following situations (stated by the testimonials gathered during the fieldwork phase of this work):

- There is a perception of adobe-based constructions as inherently dangerous and vulnerable towards seismic actions. This perception was reinforced after several official statements from the Mexican government (Zatarain 2017).
- Adobe houses are perceived as outdated for some contemporary needs.
- There is a lack of good workmanship and artisans for repairing and replicating the ancient construction techniques, and, therefore, quality work for adobe construction is often expensive when compared with more recent construction processes and technology.
- In many cases, access to public or private funds for reconstruction was subjected to the acceptance of architectonic criteria and features with no participation or intervention of the habitats and/or owners. Among others, the urgency to recover and rebuild after the seismic events leads to accepting these conditions.
- Some owners had to invest their resources in reconstruction. These resources, often very limited, were insufficient for developing a proper architectural and engineering project, making their buildings less prone to earthquake actions.

Therefore, this substitution process was accompanied by the demolition of historical structures and even buildings that could be subjected to retrofitting and strengthening actions. Furthermore, the retrofitting and/or strengthening of adobe structures were perceived as more costly and relatively useless when compared to building new structures.

This loss of cultural heritage represents a long-term impact to the detriment of both tangible and intangible assets (these constructions are the materialization of the accumulated knowledge of several generations). Moreover, this loss represents a hazard for sustaining long-term consolidated economic dynamics, such as the touristic attractiveness of some historical centres. As stated in the Historic Urban Landscape (HUL) guidelines (UNESCO 2016), the conservation of these environments is especially meaningful given the permanent nature of the loss of historical assets. For example, the municipality of Tepoztlán (State of Morelos) is very illustrative: the integration of landscape, urban, and historical architecture sustains strong cultural and ecotouristic activities that represent the main local economic activity (Alvarado and C 2015).

The study herein presented aims to explore assessment strategies for proactively identifying vulnerable constructions, admitting that prevention is preferable to reparation and substitution. This task is inscribed in

some international guidelines, such as the Chart of the Sendai Framework for Disaster Risk Reduction 2015–2030 (United Nation 2015), whose first urgent action is “Understanding Risk”, including pre-disaster risk assessments.

Furthermore, according to the “Geoethics” principles (Peppoloni and Di Capua 2021), the awareness of potential risk situations is key to having successful public policies and represents a professional responsibility for developing better practices involving a more robust social role. Hence, the vulnerability assessment of historical constructions is complementary to cultural and economic sustainability and an opportunity for a more informed and participative decision-making process towards risk mitigation.

1.3. Outline of this study

This work’s first step is based on the use of a seismic vulnerability assessment approach extensively applied in European historical cities for analysing some Mexican built environments. This approach, developed from the Italian GNDT-II method (GNDT 1993), is based on the retroactive identification of material, physical, and geometrical parameters that seem to influence the seismic behaviour of masonry constructions. Therefore, the evidence of seismic events in the last three decades allowed us to enhance, enrich, and adapt this approach, leading to different variations and calibration of parameters for different regions and several cities.

For this method’s purposes, the descriptive model of constructions considers a total of 14 parameters drawn from a straightforward survey. The first insight for applying this method was explored in the city of Atlixco, Puebla, finding the suitability of using the Mexican Catalogue of Historical Monuments for feeding the aforementioned survey (Ramírez Eudave and Ferreira 2021). Nevertheless, some limitations related to the uncertainties during data acquisition were found. A second experience with more than 80 buildings (Ramírez Eudave, Ferreira, and Vicente 2022) allowed having a better understanding of the suitability of this approach, its limitations and its possibilities.

The present study is aimed to explore the suitability of this method on a different Mexican traditional typology (that of adobe-based structures), based on the comparison between the levels of physical damage predicted by the method against the real effects, this is the observed physical damage that the 2017 Earthquake had, feeding a discussion about the representativeness of the vulnerability-oriented model and the studied built environment. Despite the VIM approach being mostly

applied to stone or brick masonry constructions, the version adopted for this study (Ramírez Eudave, Ferreira, and Vicente 2022) explicitly accepts the suitability of assessing adobe-based constructions without performing specific calibrations. This capability of the parametric method is possible since adobe is part of the vulnerability classes defined and typified in the EMS-98 approach.

Given that we accept that the set of parameters is representative for conditioning the level of damage, it is possible to accept it as a Handcrafted Feature Extraction Technique (Dash et al. 2022). This means that a series of features that can be extracted from a certain element (in this case, buildings) are valuable for predicting a certain phenomenon (such as seismic structural response). Therefore, it is possible to use this methodology as a base for training a Machine Learning algorithm to recognize potentially different configurations of the vulnerability-oriented survey that better represent this sample, leading to a new potential use of the parameter-based methodology.

2. Materials and methods

This work was performed by following a series of field surveying campaigns in four different municipalities of the State of Morelos: Jojutla, Tepoztlán, Tlayacapan and Yautepec, in which there exists a complete and relatively updated Catalogue of Historical Monuments (INAH 2019). This research is aimed to compare the level of damage that the structures had in the context of two different approaches for predicting it: a parametric vulnerability index approach (considering both, a direct and a range-based application for addressing some epistemic uncertainties) and a machine learning algorithm for finding a more suitable model based on the method’s survey.

2.1. Vulnerability Index Method (VIM): parameters and procedure

The version of the Vulnerability Index Method (VIM) herein used coincides with the one reported for Atlixco, Puebla (Ramírez Eudave, Ferreira, and Vicente 2022), in which the criteria for grading the parameters are extensively reported. Each parameter (see Table 2) is graduated in four different growing vulnerability classes (A, B, C, D) that represent how negative a given configuration is for the overall behaviour of the structure. Each grade is later associated with a numeric value C_{vi} that is later multiplied by the parameter’s weight p_i (a numerical representation of the relative relevance that the

Table 2. Vulnerability Index Method parameters, as used for Atlixco, Mexico (Ramírez Eudave, Ferreira, and Vicente 2022).

Parameters	Class (C_{vi})				Weight (p_i)	Relative weight
	A	B	C	D		
Group 1. Structural building system						50/100
BP1. Type of resisting system	0	5	20	50	2.50	16.67
BP2. Quality of the resisting system	0	5	20	50	2.50	16.67
BP3. Conventional strength	0	5	20	50	1.00	6.67
BP4. Maximum distance between walls	0	5	20	50	0.50	3.33
BP5. Number of floors	0	5	20	50	0.50	3.33
BP6. Location and soil conditions	0	5	20	50	0.50	3.33
Group 2. Irregularities and interaction						20/100
BP7. Aggregate position and interaction	0	5	20	50	1.50	10.0
BP8. Plan configuration	0	5	20	50	0.50	3.33
BP9. Height regularity	0	5	20	50	0.50	3.33
BP10. Wall façade openings and alignment	0	5	20	50	0.50	3.33
Group 3. Floor slabs and roofs						18/100
BP11. Horizontal diaphragms	0	5	20	50	0.75	4.91
BP12. Roofing system	0	5	20	50	2.00	13.09
Group 4. Conservation status and other elements						12/100
BP13. Fragilities and conservation status	0	5	20	50	1.00	6.86
BP14. Non-structural elements	0	5	20	50	0.75	5.14

parameter has among the set of all parameters) in order to obtain a weighted sum of all parameters as a global vulnerability index I_{vf}^* as per Equation 1, later normalized for obtaining a vulnerability value V (Equations 2 and 3).

An approach for estimating the damage grade $\mu_D = \{0 : 5\}$ given a certain seismic intensity is given in Eq.4. This expression includes a ductility factor for the structure $Q = \{1 : 4\}$ and represents a damage curve in which the macroseismic intensity is associated with a damage grade μ_D , conceptually framed in the EMS-98 system (Centre Européen de Géodynamique et de Séismologie 1998). A correction for the vulnerability is given in Eq. 5 for macroseismic intensities below 7.

$$I_{vf}^* = \sum_{i=1}^{14} C_{vi} \times p_i \quad (1)$$

$$I_v = \frac{I_{vf}^* \times 100}{750} \quad (2)$$

$$V = 0.592 + 0.0057 \times I_v \quad (3)$$

$$\mu_D = 2.5 + \left[3 \times \tanh \left(\frac{I_{EMS-98} + 6.25 \times V - 12.7}{Q} \right) \right] \times f(V, I); 0 \leq \mu_D \leq 5 \quad (4)$$

$$f(V, I) = \begin{cases} e^{\frac{V}{(2 \times I - 7)}} & I \leq 7 \\ 1 & I > 7 \end{cases} \quad (5)$$

A critical aspect of this approach is the correspondence between the mean damage grade μ_D and a set of discrete damage grades D_k , qualitatively characterized according to the macroscopic observed evidence of damage, as shown in Table 3. The VIM method was implemented for calculating the levels of damage that would theoretically correspond to the studied buildings when facing a seismic event with the intensity of the Puebla-Morelos earthquake (i.e., for obtaining values for μ_D).

The correlation between D_k and μ_D later permitted the comparison between the levels of damage obtained from the VIM approach against the real observed consequences (D_k) that the September 2017 Earthquake had on the assessed structures. For this purpose, the intensity information (in MMI scale) from the United States Geological Service was consulted (USGS 2017). The intensity maps for this earthquake lead to take an intensity $M_w = 7$ for the municipality of Jojutla, $M_w = 7.1$ for Tepoztlán and $M_w = 7.3$ for Yautepec and Tlayacapan (Sahakian et al. 2018). The ductility of all the structures herein analysed was based on the recommendations of the Complementary Technical Code for Seismic Design of the Building for Mexico City (Gobierno del Distrito Federal 2017), which is the reference for most of the country. This code recommends a value of $Q = 1$ for unreinforced masonry.

Table 3. Correspondence between discrete damage grades and ranges of mean damage grade.

Discrete damage grades, D_k	Range for the mean damage grades	
	μ_D^-	μ_D^+
D_0 – No damage. No observed damage.	0.00	0.50
D_1 – Slight damage. Presence of very localized and hairline cracking.	0.50	1.42
D_2 – Moderate damage. Cracks around openings; localized detachment of wall coverings (plaster, tiles, etc.).	1.42	2.50
D_3 – Severe damage. Opening of large diagonal cracks; significant cracking of parapets; masonry walls may exhibit visible separation from diaphragms; generalized plaster detachment.	2.50	3.50
D_4 – Very severe damage. Façade walls with large areas of openings have suffered extensive cracking. Partial collapse of the façade (shear cracking, disaggregation, etc.).	3.50	4.00
D_5 – Destruction. Total in-plane or out-of-plane failure of the façade wall.	4.00	5.00

2.2. Data management and acquisition framework

A Geographic Information System environment was used for storing and managing the data of this study, given the advantages of having a geographic reference for identifying each construction during the on-site campaign. The open-code and free software QGIS (version 3.12 București) (QGIS Development Team 2021) was selected for this purpose. A convenient capability of using QGIS for assembling the database was the use of the *plug-in* Mergin (Dobias, Sab Varga, and Petrik 2021), a cloud-based storage service that allows the access and edition of the QGIS file from multiple mobile devices, such as smartphones equipped with the app Input (Ramirez Eudave et al. 2023).

The survey was programmed as an attribute table for the layers that would later store the polygons corresponding to the constructions, containing a total of 68 fields for

storing field data and assessment results (see Table 4), including qualitative, quantitative, and Boolean data. Besides having this geographic database as a Geopackage file, a python-based front-end was programmed for performing reading and edition actions on the database. This front-end component integrates the possibility of calculating the vulnerability index and the levels of damage based on the parameters stored in the GIS database. The purpose of this script is to facilitate data management and calculations while keeping the integrity of the primary database (see Figure 2).

2.3. Characterization of the sample and field surveying

Given the affinity of the National Catalogue of Historical Monuments regarding the parameters

Table 4. General composition of the QGIS layer attribute table.

Type of fields	Number of fields	Data content
Identification	2	Address and unique primary key.
Building parameters	41	Geometrical and material features are considered for the grading of the parameters of the VIM.
Seismic parameters	1	The seismic intensity in the EMS-98 scale.
Quality Check	14	Index for grading the level of uncertainty related to each parameter.
Results	10	Storage of the vulnerability index, intermediate and final results.
Total	68	

The screenshot displays the 'Seismic Vulnerability Calculator and Database for MORELOS, MÉXICO (Sept. 2017 Earthquakes) v. 2.0 (08/22) - Rafael RAMÍREZ EUDAVE' application. The main window is divided into several sections:

- Input Form:** A grid of fields for entering building data. Fields include 'QGIS Key' (2.0), 'CNMH No. + Address' (015 Pedro Baranda 207), 'QC Help', 'Conservation' (Bad), '0a.Type of masonry' (C), 'MMI' (7), '0d.Height' (4.0), '0b.Type of diaphragm' (E), 'Q' (1), '0e.Storays' (1.0), '0c.Roofing system' (E), '2017DK' (5), and various 'BP' (Building Parameter) fields like 'BP1_Type and org. res. syst.' (D), 'BP2_Quality resisting syst.*' (D), 'BP3_Conventional strength*' (A), 'BP4_Max. dist. walls*' (D), 'BP5_Number of floors' (A), 'BP6_Soil conditions*' (C), 'BP7_Aggregate position' (D), 'BP8_Plan configuration*' (D), 'BP9_Height regularity' (B), 'BP10_Openings alignment' (A), 'BP11_Qty. Horiz. Diaph.' (D), 'BP12_Roofing System*' (D), 'BP13_Conserv. State' (D), and 'BP14_Non-struct. elem.' (A). There are also numerical input fields for 'L_vf' (575.0), 'L_vf_c' (595.0), 'L_v' (76.67), 'L_v_c' (79.33), 'V' (1.03), 'V_c' (1.04), 'Mu_d' (4.37), 'Mu_d_c' (4.54), and 'DK' (5).
- Geopackage file:** A section with a 'Load data' button and 'About' and 'Exit' buttons. It contains instructions: 'Parameters in RED can be automatically obtained having all those in BLACK fulfilled' and 'The vulnerability index can be automatically calculated having all BLACK and RED parameters'. It features 'Update', 'Reset', 'Update and run ML', and 'Run AI' buttons.
- Results Table:** A table with columns: Key, Address, Mu_d, Mu_d_c, DK2017, DK, and DKc. The first row is highlighted in blue: Key: 2.0, Address: 015 Pedro Baranda 207, Mu_d: 4.37, Mu_d_c: 4.54, DK2017: 5, DK: 5, DKc: 5. Other rows include: 3.0 025 Sor Juana Ines de la Cruz 109, 4.0 026 Covarrubias 101, 5.0 028 Zayas Enriquez 123, 7.0 034 Jesús H. Preciado 102, 9.0 038 Francisco Javier Mina no. 75, 10.0 040 Francisco Javier Mina no. 203-, 11.0 042 Francisco Javier Mina no. 101, 12.0 043 Francisco Javier Mina no. 102, and 14.0 048 Himno Nacional no. 102.
- Suggested grades:** A section at the bottom with the text: 'Suggested grades according to the given data: BP2: D BP3: A BP4: D BP6: C BP8: B BP12: D Regular: Expected damage D4: Very severe. Extensive cracking and localised collapses. Conservative: Expected damage D4: Very severe. Extensive cracking and localised collapses. Interval of damage 0:[0-0.50], 1:[0.50-1.42], 2:[1.42-2.50], 3:[2.50-3.50], 4:[3.50-4.00], 5:[4.00-5.00]'.

Figure 2. Screenshot of the python-based front-end (Ramirez Eudave 2022).

Table 5. General description of the housing environment for the studied municipalities according to the Census of 2014 (undefined).

Municipality	Number of housing units	Adobe-based housing units	Proportion
Jojutla	3705	83	2.24%
Tepoztlán	3866	423	10.94%
Tlayacapan	2246	451	20.08%
Yautepec	3927	95	2.42%
Total	13744	1052	7.65%

Table 6. Number of buildings/cases considered per municipality.

Municipality	Indicative list (obtained from the NCHM)	Effective building case records used	Percentage
Jojutla	68	55	80.89%
Tepoztlán	47	37	78.72%
Tlayacapan	34	33	97.06%
Yautepec	49	42	85.71%
Total	198	167	84.34%

considered in the VIM, those municipalities with the larger samples of catalogued buildings were selected. Among these municipalities, those whose entries in the Catalogue were completely fulfilled were preferred: Jojutla, Tepoztlán, Tlayacapan, and Yautepec. It is important to note that only constructions destined to housing were considered for this study, discarding other historical structures such as churches, agricultural complexes or other industrial facilities. Although the presence of adobe constructions in these municipalities is variate (Table 5), the assets considered in the National Catalogue of Historical Monuments (i.e., constructions built before the year 1900) are predominantly adobe-based constructions.

An original indicative list of 198 constructions was prepared, as shown in Table 6. These constructions were visited to perform visual inspections to accomplish the vulnerability survey and correct any outdated information from the National Catalogue of Historical Monuments (NCHM). This campaign led to the exclusion of several constructions (for example, some buildings were inexistent or structurally heavily modified when the earthquake hit) profiling a final universe of 167 valid cases that were characterized, stored, and analysed.

The fieldwork allowed the accomplishment of a series of activities:

- (i) Visual confirmation of the descriptive information contained in the National Catalogue of Historical Monuments. The position of the construction was confirmed or corrected. Then, the information contained in the Catalogue was

compared against the field data gathered, leading to corrections, if necessary.

- (ii) Photographic register of the interior and exterior. All constructions were at least registered by the exterior. In many cases, access was not allowed or restricted. When access was not permitted, the interior description of the constructions was based on the content of the National Catalogue of Historical Monuments. It is convenient to recall that only buildings with a complete datasheet (i.e., with architectonic floor plan, photographs, and descriptions) were considered valid samples during the preliminary selection.
- (iii) Damage questionnaire to the owners/users of the constructions. Besides communicating the goal and procedure of the fieldwork, the users were asked to describe the type of damage that structures had after the 2017 Earthquakes. The diagram that illustrates the classification of damage to masonry buildings in the EMS-98 scale (Centre Européen de Géodynamique et de Séismologie 1998) was shown to better classify the level of damage (see Figure 3).
- (iv) Geometrical measurements (e.g., exterior measures for contextualizing the architectonic plan drawing of the Catalogue).
- (v) Register of information for grading vulnerability index parameters.

Many of the fields were able to be directly registered on-site by using the app “Input” for editing the GIS database. In some cases, quantitative vulnerability index



Grade 1: Negligible to slight damage (no structural damage, slight non-structural damage).

Hair-line cracks in very few walls.
Fall of small pieces of plaster only.
Fall of loose stones from upper parts of buildings in few cases.



Grade 2: Moderate damage (slight structural damage, moderate non-structural damage).

Cracks in many walls.
Fall of fairly large pieces of plaster.
Partial collapse of chimneys.



Grade 3: Substantial to heavy damage (moderate structural damage, heavy non-structural damage).

Large and extensive cracks in most walls.
Roof tiles detach. Chimneys fracture at the roof line; failure of individual non-structural elements (partitions, gable walls).



Grade 4: Very heavy damage (heavy structural damage, very heavy non-structural damage).

Serious failure of walls; partial structural failure of roofs/floors.



Grade 5: Destruction (very heavy structural damage)

Total or near total collapse.

Figure 3. EMS-98 five damage grade scale (Centre Européen de Géodynamique et de Séismologie 1998) and examples of buildings with corresponding damage grades from 1 to 5 in the studied municipalities.

parameters were able to be graded only after performing some calculations, assisted by the python-based front end.

Although there is a certain variability throughout the sample, most of the assessed constructions (see Figure 4) share several characteristics.

The vernacular typologies found in these municipalities are common to most of the State of Morelos and present little variations (Quintana Leonardo and Guerrero Baca Luis 2010). These houses commonly consist of a single-storey level (ground) room with a rectangular plan configuration for rural areas, whilst



Figure 4. Examples of urban (left) and rural (right) houses.

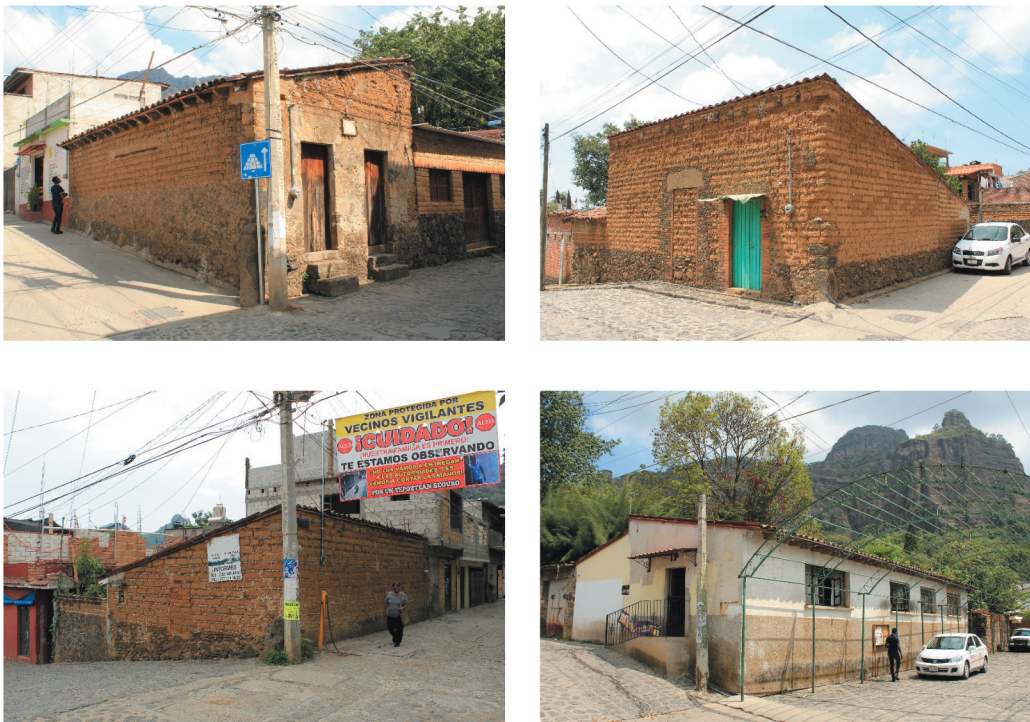


Figure 5. Typologically representative constructions from the municipality of Tepoztlán.

urban houses present a series of rooms of similar sizes, internally connected and aligned with the street (Figure 4).

The most common structural solution is one-leaf adobe walls built with units of ca. 52 cm in length, 36 cm in width, and 9 cm in thickness. Although there are no additional means of reinforcement or strengthening, there is good interlocking and layering and most constructions have visible stone foundations. Most foundations reach a height of between 0.50 and 1.00 m from the level of the street, mainly as a strategy for isolating the adobe walls from the soil humidity and rainwater (Figure 5). The most common roof solution is a plane-pitched roof that facilitates rainwater collection by the means of dedicated ceramic pipes. The openings in

these constructions are proportionally small, solved by means of timber lintels or stilted arches.

The adobe walls present earth-mortar joints in which small ceramic pieces or stones are embedded to offer better protection (Figure 6). The adobe units are visibly homogeneous, and only two elements are easily recognizable: the earth matrix and fine vegetal fibre elements.

All the local inhabitants that were inquired about the typical constitution of adobe bricks described the production of adobe from a mixture of the soil available onsite and horse manure that is compressed in wooden formworks and sun-dried. Even if many of the constructions have no external render, the inhabitants often state that this is a relatively recent tendency,

mostly for offering an attractive “rural” visual landscape for tourism purposes.

The physical damage of the number of structures assessed was classified as per the EMS98 scale and is summarized in Table 7.

3. Results and discussion

The results analysis for this experiment had three main stages. The first approach consisted of a direct comparison between the observed damages and the mean damage grade estimated using the seismic vulnerability index approach. A second stage of analysis considered some limitations found during the field-work campaign and, finally, a third stage considered the use of Machine Learning algorithms for assessing how suitable is its use for predicting the levels of damage and calibrating the weights of the Vulnerability Index Method for specific typologies and built environments.

3.1. Simple parameter-based analysis

It is important to note that the qualitative scale for classifying the observed post-seismic damages on structures corresponds to intervals for mean damage grade μ_D . The first comparison for assessing the suitability of the method on the given number of building cases consisted in checking if the analytical value obtained for μ_D was comprised in the permissible range of the real/observed damage $D_{k,2017}$ (see Figure 7). A total of 104 out of the 166 cases (62.28%) present coincidence

between the predicted μ_D and observed $D_{k,2017}$ levels of damage (see Table 8).

When the method fails at predicting the level of damage, it is often an underestimation of it (i.e., analytical levels of damage were less severe than the real damages observed and described in situ). It should be noted that the semantic descriptors used in the VIM approach for modelling the built environments (type of structures, materials, etc.) were enough for describing the buildings herein presenter. Nevertheless, it is pertinent to consider that some relevant phenomena or characteristics may not fit in this survey model.

For example, despite the general conservation status of the construction being a parameter assessed for determining the vulnerability to seismic actions, earth-based structures may have more specific deterioration issues and fragility due to moisture content in structural elements. This specific defect is not included in the original approach but can intuitively be significant for assessing the state of construction. This observation becomes even more relevant when considering the number of constructions that had lost the external renders for aesthetic reasons. This discussion is not further developed in the context of this article since the moisture content of the constructions at the moment of the earthquake is unknown. Nevertheless, it provides an opportunity for discussing, enriching, and adapting the VIM survey for future experiences.

Another reasonable explanation for this lack of representativeness is related to a condition that worsens the structural behavior, such as an unfavourable soil-structure interaction. Besides, a certain grade of unrepresentativeness can be a consequence of the limitations



Figure 6. Typical adobe configuration in a house in the municipality of Tlayacapan.

for having reliable data acquisition, namely, due to field restrictions (inaccessibility, lack of safe conditions for performing field works, etc.).

3.2. The role of uncertainty

Given the access limitations during the fieldwork and the consequent uncertainties in the evaluation associated with certain parameters, it was decided to take into account the Quality Check (QC) approach proposed for the city of Atlixco (Ramírez Eudave, Ferreira, and Vicente 2022). This approach adds a code for each parameter to express how reliable the data acquisition process (and, therefore, the grade assignment) was.

The four possible values for the QC are:

QC0: High reliability. Grade verified with a high level of certainty. Data are explicitly contained on the data-sheets and have been verified in situ.

QC1: Medium reliability. Deduced from secondary sources, (photographs, drawings, testimonies, etc).

QC2: Low reliability. Inferred based on typological similarities and hypothesis based on experience.

QC3. Absence of information. The grade is merely indicative but still better than a random decision.

Parameters for which the reliability of the evaluation was considered to be QC0 or QC1 level, no further action is taken and the vulnerability classes assigned for that parameter are accepted. Otherwise, the hypothesis of having a lower vulnerability class than the initially proposed is sustained. Therefore, an alternative conservative assignation of the vulnerability class is adopted by downgrading one or two classes, respectively, for QC2 and QC3 (e.g., from A to B or from A to C). As an example, in a construction for which access

was not granted, the surveyor may decide that the inner conservation status (assessed by parameter BP13) is good, according to typological similarities and previous experiences. But, since no visual confirmation was possible, a QC2 reliability level must be assigned to this parameter. This means that the vulnerability-oriented survey will initially consider BP13 with a grade A, whilst the conservative boundary of the vulnerability index will be calculated assuming that this same parameter can have a grade B (or C, in case of having a QC3).

Therefore, the mean damage grade μ_D becomes an interval with two boundaries: a lower limit that corresponds to the vulnerability class initially given during the field campaign and an upper limit that correspond to a more conservative assessment in which the uncertainties have been considered, as the safe side definition.

This approach is possibly easier to understand when expressed graphically, as shown in Figures 6 to 13. For each building, the boundaries for the analytical damage range, μ_D and $\mu_{D,conservative}$ (obtained by applying the VIM), are represented through a black horizontal bar and a cross, respectively, while the intervals for the discrete qualitative observed damage grades assigned (the real damages observed in the building) are represented through a white bar, facilitating the interpretation of the overlapping among both intervals.

With this approach, the vast majority of predicted damage intervals overlap with the corresponding intervals of observed damages (see Table 9). This observation is consistent with the results reported for Atlixco, supporting the feasibility of the joint use of an alternative and more conservative value for assigning an interval for the physical damage instead of closed and nominal values.

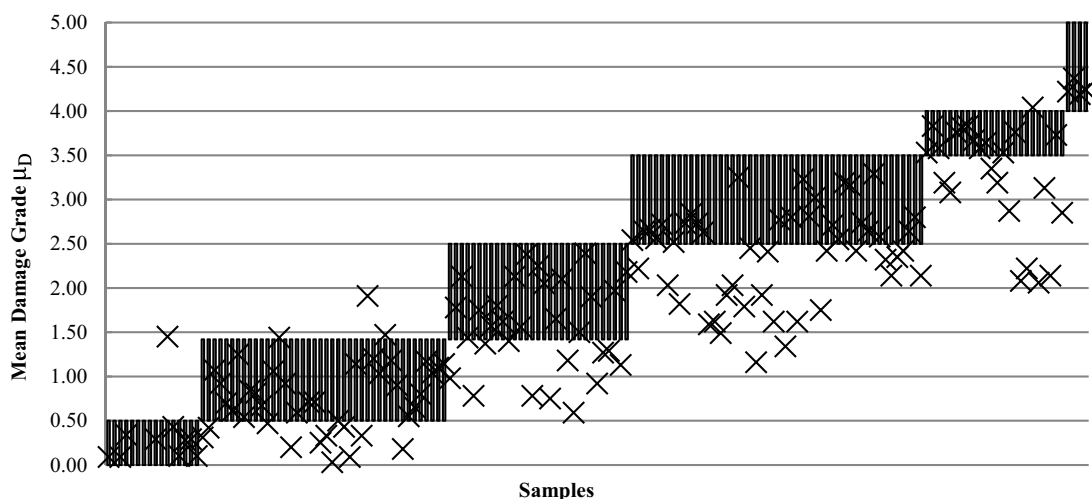


Figure 7. Comparison between the intervals for the permissible range of observed damage (bars) and analytical damage (black crosses) by sample.

Table 7. Number of structures assessed by municipality and level of damage.

Municipality	$D_K = 0$	$D_K = 1$	$D_K = 2$	$D_K = 3$	$D_K = 4$	$D_K = 5$
Jojutla	3	5	3	26	17	1
Tlayacapan	3	7	7	11	4	1
Yautepec	5	15	9	10	2	1
Tepoztlán	5	15	12	3	1	1
Total	16	42	31	50	24	4
	9.58%	25.15%	18.56%	29.94%	14.97%	2.40%

Nevertheless, this approach does not solve the potential lack of representativeness associated with the conceptual models used in the VIM approach. Even if the calibration and adjustment of the methodology by means of analytical approaches are possible, the experience herein presented explores the suitability of resorting to machine learning tools for predicting the damage grades from the set of parameters already acquired, unveiling hidden patterns and potential redistributions of the weights originally proposed.

3.3. Machine learning approach

The use of trained algorithms for recognizing patterns and subjacent relations has been demonstrated to be suitable for numerous problems in which the relations between input data and outcomes (results) still present hidden or not well-defined mechanisms. Given that the proposed procedure is intrinsically attached to a regressive analysis of cause-effect elements based on categories (both for the parameters and the damages), the use of computational analysis is a strong and suitable measure for expanding the boundaries of this methodology.

It is important to note that the VIM approach is based on an existing empirical parameter-based methodology built on the evidence of past events: the analysis from numerous seismic events, the classification of the structures and their damages, representing a process of domain knowledge Handcrafted Feature Extraction. This process is critical for recognizing which descriptors (features) are more important for determining an outcome (Guyon and Elisseeff 2006). For the case of the seismic vulnerability of masonry structures, this feature extraction has been empirically conducted and refined based on numerous observations, leading to determining the set of 14 parameters used in this investigation. This approach is a response to the limitations that robust structural analysis (strongly customized in the case of historical structures) has when dealing with large numbers of buildings or constructions to be assessed.

3.3.1. Machine learning principles

Although the use of Machine Learning and Deep Learning approaches (subfields of Artificial Intelligence) for studying complex processes is not new, their use in the context of complex civil engineering applications is not generalized yet. A relatively recent field of application of Machine Learning algorithms is the health monitoring of historical structures and heritage buildings, in which heterogeneity, complexity, and variability are still relevant challenges for more generalized approaches (Mishra 2021).

The use of these resources should always be accompanied by awareness regarding their limitations, bias and the limits of the control that the user has towards the several “black boxes” that these processes imply (Vadyala et al. 2022). It is possible to obtain apparent accurate predictions and structured models even from weak evidence and scarce data. Therefore, to have a robust control of the representativeness of input data, the integrity of data and the correct selection of models and cases are critical aspects to consider. In this case, the existence of a precedent data model (that of VIM) is useful for contextualizing the results obtained when performing the Machine Learning algorithm design and assessment.

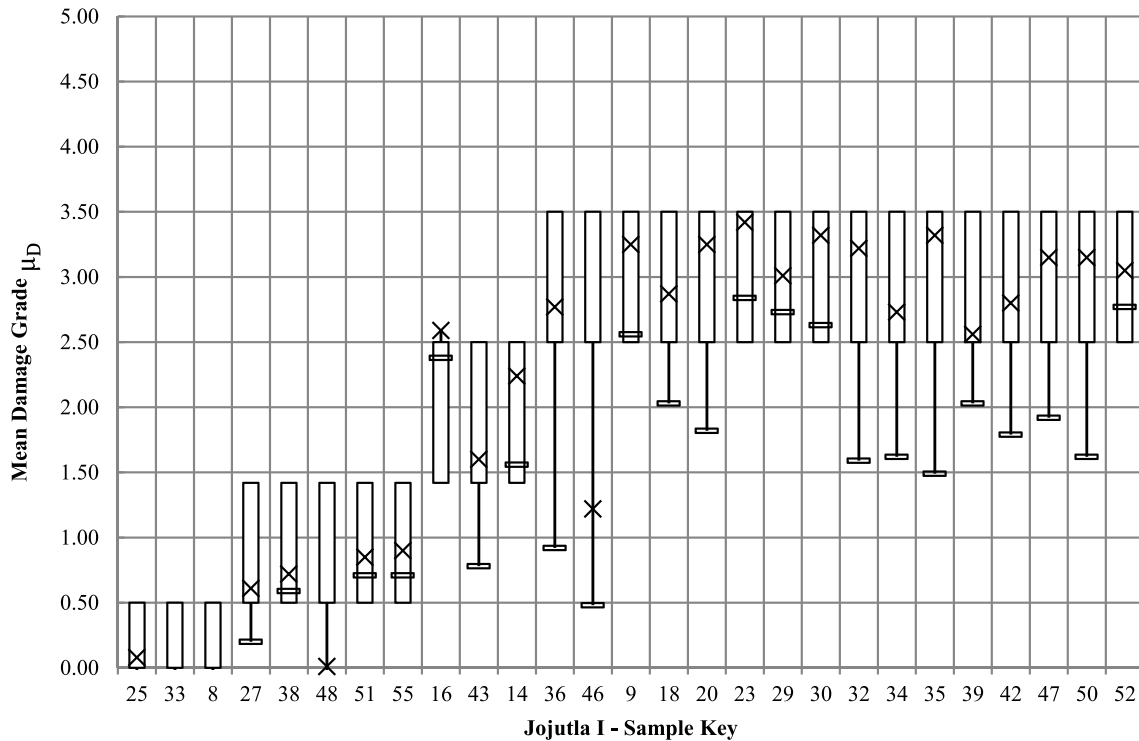
3.3.2. Implementation

The approach adopted for this case study accepts a series of assumptions related to the type and quality of data. The most important one is that the labelling of the input and outcome data has been directly adopted from the VIM methodology. In other words, the parameters, grading, and levels of damage have been adopted as is, so the database used in the previous sections did not suffer alterations.

The general workflow herein presented is that proposed in the documentation of the freeware learning library *scikit-learn* (Pedregosa et al. 2012). This library supports many of the most common classification, regression, and clustering algorithms for Python programming environment, namely through the *NumPy*

Table 8. Summary of successful predictions for the level of physical damage.

Municipality	Successful	Failed	Success ratio (%)
Jojutla	27	28	49.09%
Tepoztlán	28	9	75.68%
Tlayacapan	19	14	57.58%
Yautepec	30	12	71.43%
Total	104	63	62.28%

**Figure 8.** Analytical and real damage grade intervals for the municipality of Jojutla (1 of 2).

library. The implementation herein presented was programmed as part of the database front-end manager to work within the original database (Ramirez Eudave 2022).

3.3.3. Importing data

The vulnerability database was built in a GIS environment using Geopackage files in native format. Thus, the management of the database was held by means of GeoPandas, a Python open-source library that supports the management of geospatial information as well as more typical non-geographical data frames. This library allows the management of GIS native files (Geopackages, shapefiles, etc.) as tabular data keeping the integrity of georeferenced information. Therefore, these capabilities allowed us to read and import the

database, namely the 14 parameters (and their associated vulnerability classes).

For this process, it becomes critical to assign labels and recognize which components of data represent features and target outcomes. In other words, it is necessary to identify which data is meaningful for conditioning the outcome. For example, the database includes the address of the constructions, an information that is not critical to explain the level of physical damage of the structure. Nevertheless, this dataset already contains 14 labelled parameters (the labels are the parameters' classes) that we already consider valid for defining and estimating the level of damage (i.e., the outcome) of a structure in the context of a determined earthquake. The process of recognizing these features is part of the so-called Handcrafted Feature Engineering,

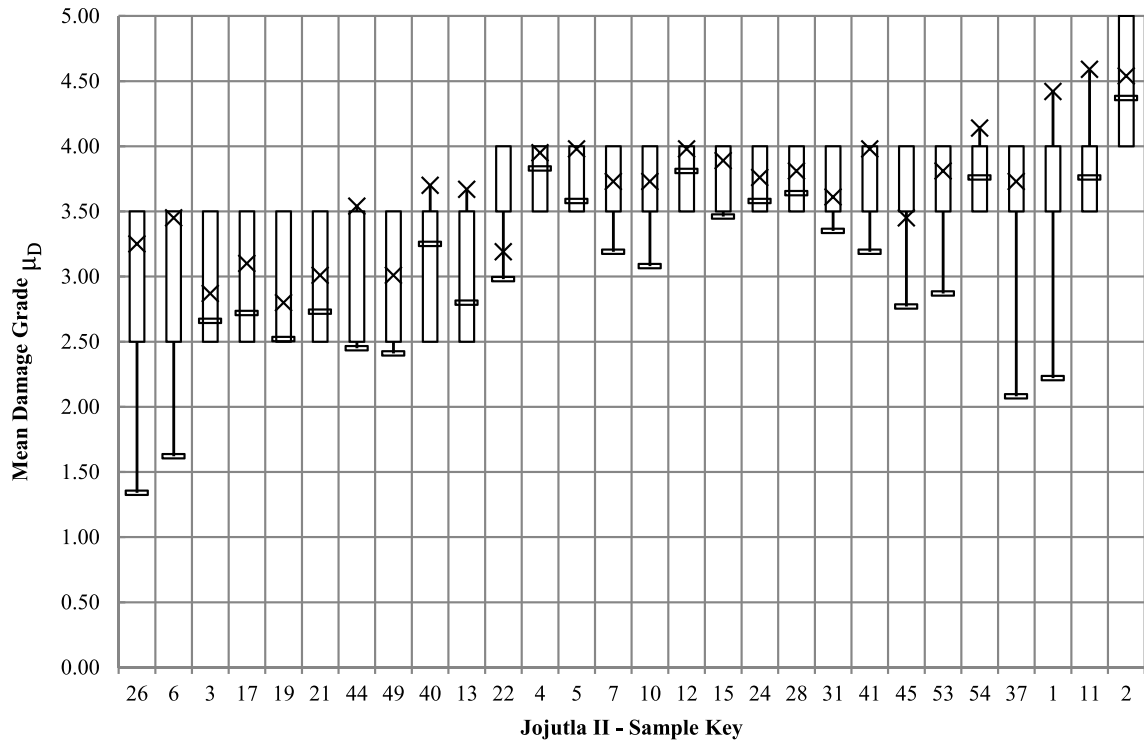


Figure 9. Analytical and real damage grade intervals for the municipality of Jojutla (2 of 2).

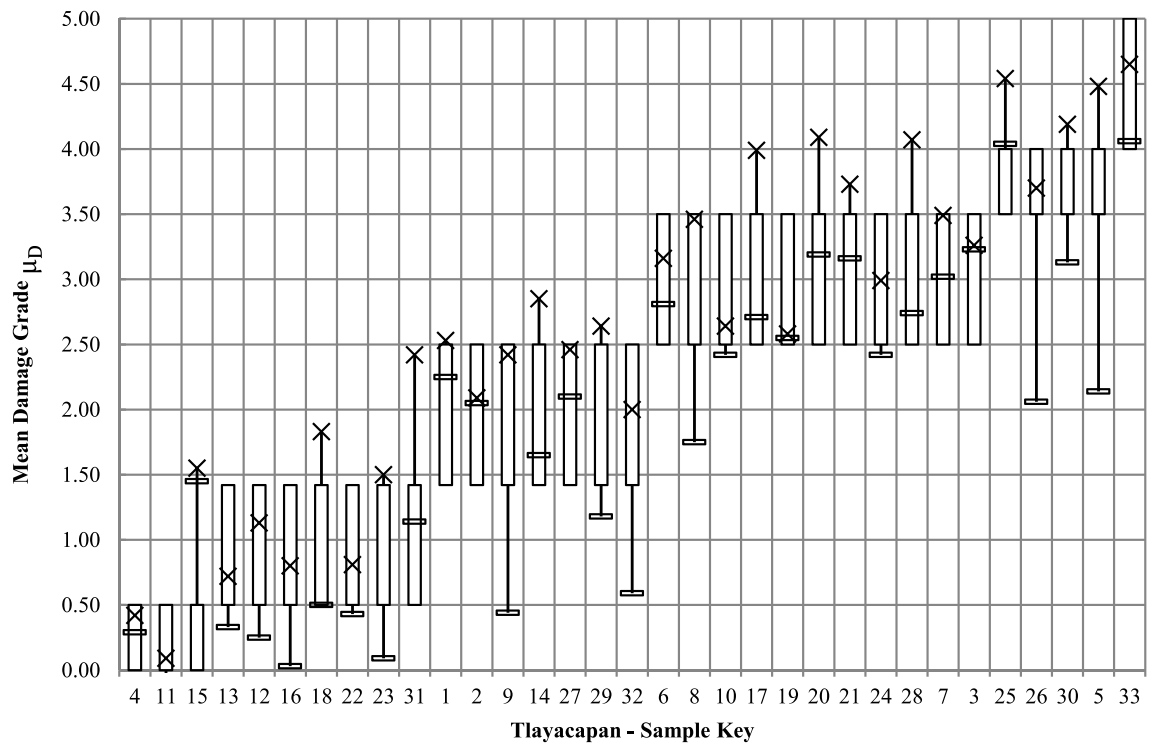


Figure 10. Analytical and real damage grade intervals for the municipality of Tlayacapan.

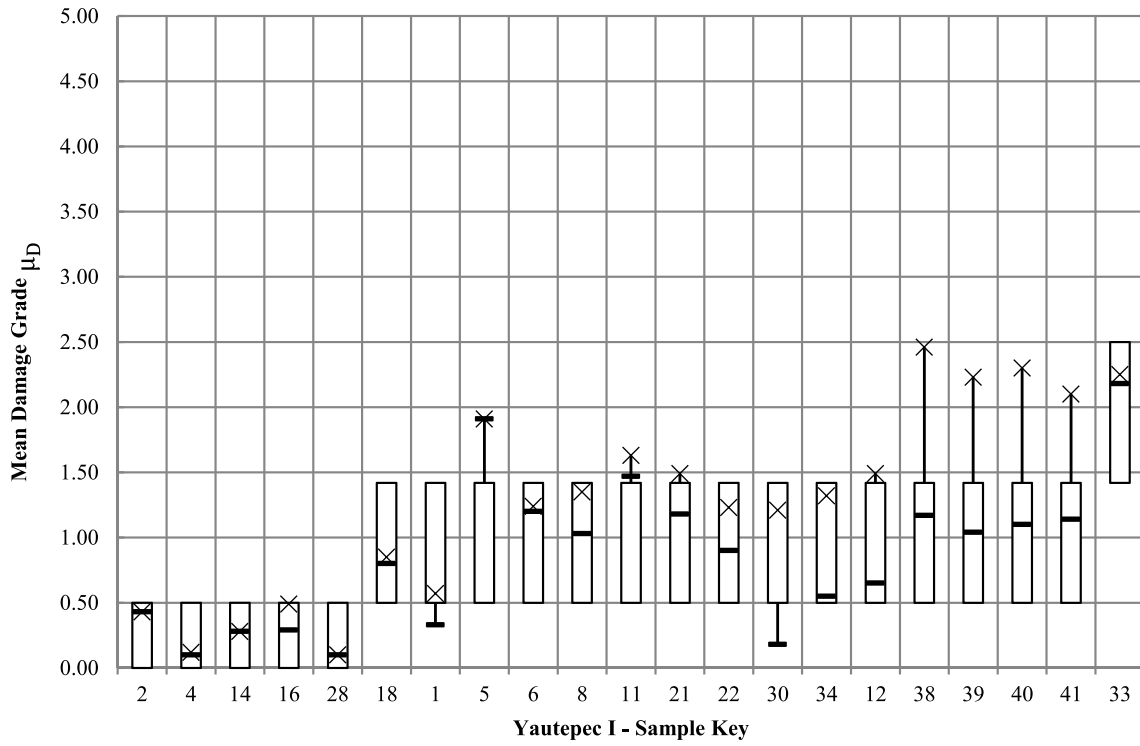


Figure 11. Analytical and real damage grade intervals for the municipality of Yautepec (1 of 2).

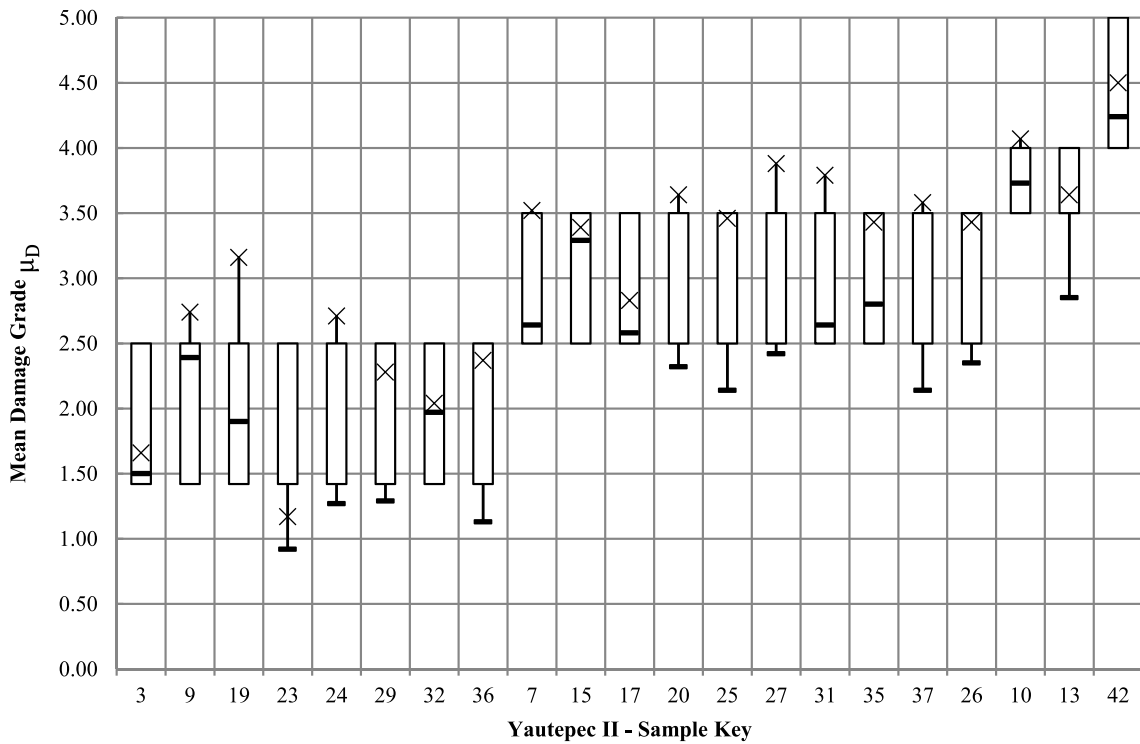


Figure 12. Analytical and real damage grade intervals for the municipality of Yautepec (2 of 2).

which can otherwise be performed by the means of domain knowledge or other approaches.

Given that this process is an inherent part of assuming the VIM methodology, all the 14 parameters considered in the database are meaningful for defining the level of physical damage (outcome) of the structure. Nevertheless, in contrast to the VIM approach, the ML algorithm does not assess the parameters from a given weighted importance (i.e., the only information the algorithm has is that the parameters are related to the outcome). Instead, the ML algorithm will fit a distribution of weights per parameter that represents a more fitted and representative model.

This clarification is especially relevant because, in contrast, some ML processes are also aimed at the identification of learned features from raw data (Khurana, Samulowitz, and Turaga 2018).

3.3.4. Cleaning and splitting data

This step was performed in the scope of input data presented in sections 3.1 and 3.2, in which the integrity of the database and the completeness of entries were verified. According to the good practices reported in similar classification problems, 20% of data were reserved for performing verification tests. This fraction may vary according to several criteria and the size of the sample, but common practices in

this field often accept an interval of 15–20% as a reasonable ratio.

3.3.5. Creating a model (algorithm selection)

The selection of a suitable algorithm is one of the most critical steps for representing a problem with Machine Learning tools. For this exercise, a Supervised Learning approach (i.e., data for training associates sets of features with specific outcomes that are expected to further predict new sets of features) was carried out. Given that the target outcome consists of discrete damage grades (a level of damage $D_K = \{0, 1, 2, 3, 4, 5\}$), the model has been categorized as a classification problem (i.e., data is labelled with two or more classes and the Machine Learning processes would find valuable vectors for pointing outcomes from the labelled features. As schematized in Figure 14, the field dataset (the 166 observations that include the parameter's grading and the real post-seismic levels of damage) is used for training the RFC algorithm, so the algorithm recognizes patterns between the parameters and the levels of damage. This trained model replicates these patterns for predicting the outcomes that can result from a given combination of parameter grades. The prediction can be used for obtaining outcomes from new samples and/or assessing the accuracy of the model by predicting already-known outcomes. In this case, 20% of the data was reserved for performing this assessment process.

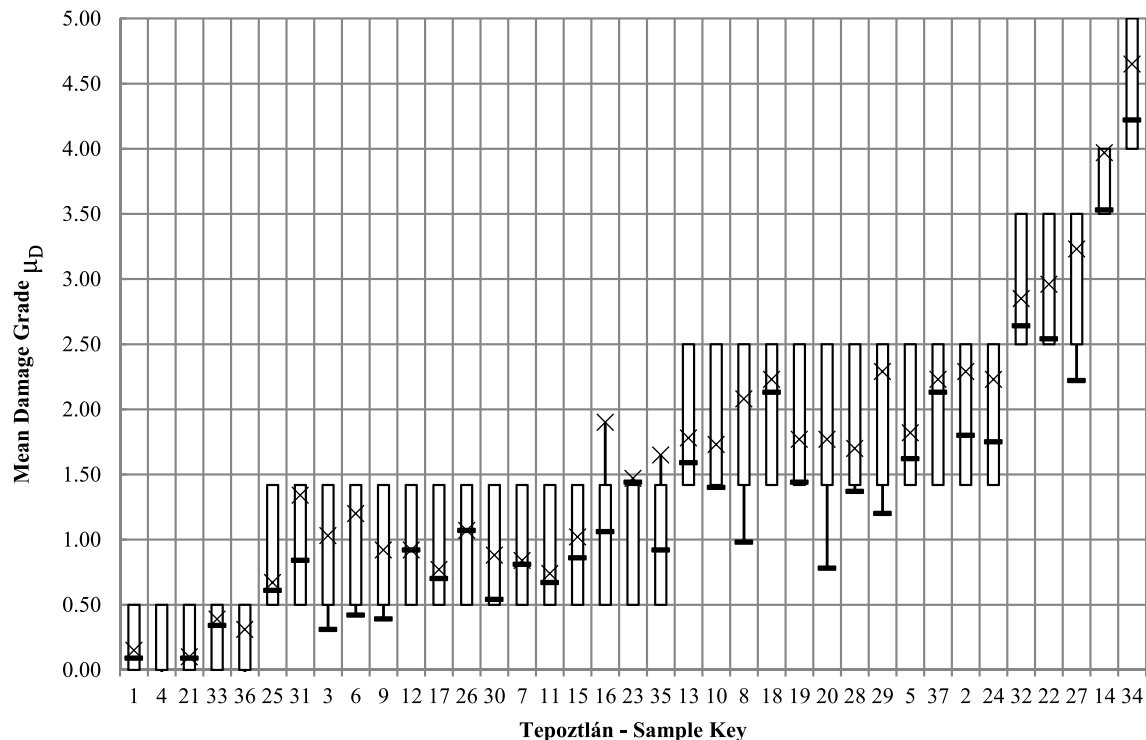


Figure 13. Analytical and real damage grade intervals for the municipality of Tepoztlán.

Table 9. Summary of samples in which the observed and estimated damages are overlapped.

Municipality	Successful	Failed the criteria	Success ratio (%)
Jojutla	50	5	90.91%
Tepoztlán	34	3	91.89%
Tlayacapan	32	1	96.97%
Yautepec	40	2	95.24%
Total	156	11	93.41%

The problem herein presented is a classification and regression task since the parameters are given but their relative impact on the outcome is not provided to the algorithm. If some parameters (features) of the income data are not useful, this algorithm minimized/reduces its relative sensitivity on the model.

By following the observations of (Buitinck et al. 2013), this problem can be modelled by the means of the Random Forest Classifier (RFC) learning algorithm. This algorithm ensemble numerous decision trees (i.e., flowchart models in which an outcome is a product of a specific path of several conditional statements or nodes) that fit fractions of data instead of creating a unique tree model. This algorithm prevents model overfitting by using multiple trees and the so-called bagging method. As schematized in Figure 15, the bagging process consists in randomly splitting the complete dataset into a series of equally sized datasets. Since the selection is randomized, each observation can appear in more than one tree. The number of trees is not limited by the number of observations of the dataset. Each subset is used for training a customized individual decision tree (i.e., for fitting a partial model based on the subset of observations). When a new observation is introduced to the model, each tree “votes” according to its particular training. The complete model assigns an outcome based on the overall “votes” of the partial decision trees. The sum of all these random trees represents the so-called “Random Forest”.

Among the many available algorithms for performing classification works, the RFC was considered especially suitable because does not make assumptions about the underlying distribution of data and because it permits a better understanding of the relative influence that the features have (assuming that all the selected features are meaningful).

Given that this classification problem departs from an already-established survey (that has been tested, calibrated, and enriched based on the evidence of multiple seismic events) instead of raw data, we accept that all the features are valid and influence the outcome. There is a subjacent decision-tree structure for the VIM analytical procedure. The conceptual compatibility between the

analytical development of the VIM approach and the RFC is therefore considered key for comparing both techniques.

The application of RFC for modelling seismic vulnerability-related phenomena has some relevant precedents, such as the mapping based on damages after seismic events (Han et al. 2020), post-earthquake reconnaissance for reinforced concrete structures (Midwinter, Yeum, and Kim 2022) and structural elements damage models (Lei et al. 2020).

3.3.6. Training the model, making predictions and evaluating the model

The model herein presented was trained using the hyperparameters (parameters whose values control the learning process and determine the values of model parameters that a learning algorithm ends up learning) setup summarized in Table 10. No relevant characteristics of the dataset seemed to be critical for rejecting the default settings, except the number of trees, which was set according to the observations of (Oshiro, Perez, and Baranauskas 2012). Given the nature of this classification problem (a relatively simple one), no further adjustments were needed.

A series of predicted classifications were obtained by using the data reserved for testing the model (34 random samples), integrating a new data frame that allowed the comparison between the real outcomes (the $D_{K, 2017}$ levels of damage) against those predicted by the model (Figure 16).

This process allowed us to understand how representative and effective the model is. The metrics for evaluating the model were obtained by using the classification report embedded in the Sklearn package (see Table 11). This report offers three main metrics for each class:

- Precision. The ratio of successful identifications of a class divided by the number of times that the label was predicted in the model. This is the ratio of the true positives divided by the sum of true and false positives.
- Recall. The ratio of successful identifications of a class divided by the number of samples that

belong to that class. This ratio expresses how many relevant identifications were retrieved.

- (c) F1-score. Represent the harmonic mean between precision and recall, representing the performance of the model.

An explicit representation of the results is the confusion matrix, in which the correspondence between the true and predicted labels (i.e., discrete levels of damage) is shown in Figure 17. This confusion matrix exhibits how most of the classes were correctly identified by the model, but there is a lack of representativeness in identifying the highest level of damage $D_K = 5$. This phenomenon can be easily associated with the relatively small number of samples used for training purposes in this class (4 out of 167, 2.4%; however, it appears only once in the test split of the sample) since this is the most infrequent class, it is expected to be less likely recognized by the algorithm.

It is possible to retrieve which is the relative impact that every parameter has in the classification process. At this point, it becomes convenient to be aware of the limits imposed due to the variability throughout the sample, i.e., the impact of a determined parameter will be smaller if it does not present relevant variations for differencing samples. The sample herein studied presented relatively small variations in some parameters given the typological coherence amongst the structures (Figure 18). The feature importance (see Figure 19) of the model reflects this phenomenon.

The model for this sample exhibits relatively low importance for certain parameters, such as BP3 (Conventional strength), BP5 (Number of floors) and BP14 (Non-structural elements), which is consistent with the typology observed in situ: one-storey constructions with no remarkable features in the facades and with similar plan distributions. On the other hand, parameters such as BP2 (Quality of the resisting system), BP7 (Aggregate position) and BP13

(Conservation state) are critical for assigning a vulnerability class. Regardless of the physical meaning of these parameters, the algorithm identifies that BP2, BP7, and BP13 seem to have a more consistent effect in the outcomes, and it determines that these parameters are strongly conditioning the results. It is convenient to recall that, therefore, this weight distribution can be seriously limited when analysing a very different typology that would become an “outlier”, such as a building with more than three storeys.

The most obvious way for improving this approach is to enlarge the dataset to enhance the representativeness of extreme values. The generation of synthetic data under the assumption of normality was considered. To check the suitability of this approach (e.g., by using Montecarlo or Latin Hypercube sampling methods), the normality of the distribution of the observed level of damage was assessed by the means of the Kolmogorov–Smirnov test. The normality hypothesis H_0 is not supported at a significance level $\alpha = 0.05$, obtaining P -values < 0.00001 and, therefore, this experiment is not suitable based on the existing evidence and the dataset was not enlarged. This procedure would have been useful for enlarging the dataset without losing its representativeness and having a larger number of extreme observations. It is important to keep in mind that larger datasets obtained in situ may provide evidence for finding representative statistical distributions for the levels of damage.

4. Final remarks and future work

This work presents a series of processes based on the vulnerability assessment of structures damaged as a consequence of the 2017 earthquakes in the centre of Mexico. A total of 167 constructions were surveyed to obtain a set of 14 parameters that allowed the estimation of vulnerability index and consequently the

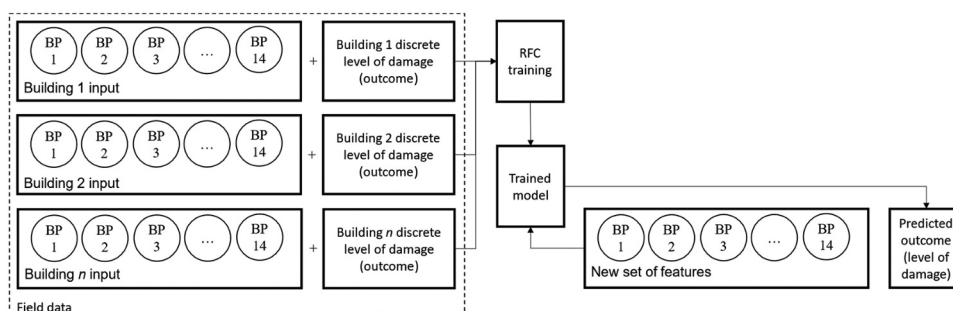


Figure 14. Flow diagram of the training and prediction processes.

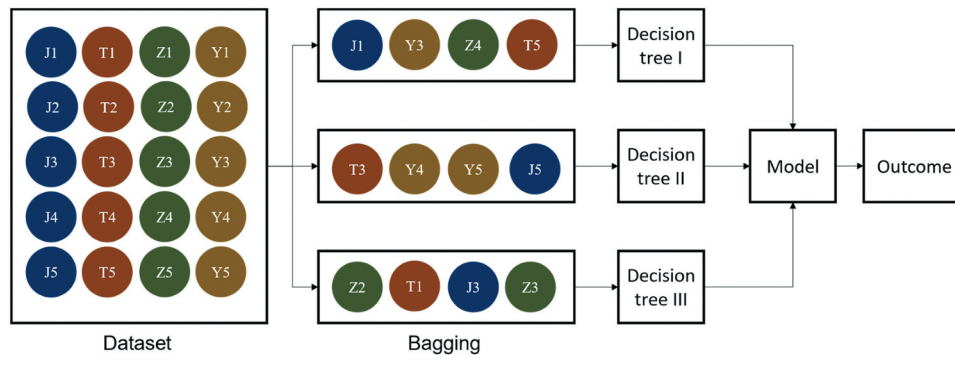


Figure 15. Schematization of the bagging process.

determination of mean damage grade when subjected to a determined intensity earthquake.

The sample herein presented corresponds to a typologically homogeneous housing dataset distributed throughout four municipalities of the State of Morelos, emphasizing the predominance of adobe-based structures. All the constructions were surveyed in situ, accomplishing a database containing the pre-seismic characteristics of the buildings. This process was possible with the support of the National Catalogue of Historical Monuments, interviews with the building owners and users and visual in-situ inspections. The level of physical damage that every construction evidenced/experienced was compared with the predicted level of damage according to the VIM methodology.

A first attempt consisted of the direct application of the method, neglecting some sources of uncertainty identified during the surveying campaign (incompleteness of information, the impossibility of accessing all constructions, etc.), resulting in a 62.28% of acceptable agreement (i.e., the estimated damage was comprised with an interval of the real/observed damage).

A second exercise was developed by enriching the method with the addition of a quality check in which the uncertainty for assigning a certain vulnerability class is accepted and integrated for obtaining an alternative, more conservative, level of physical damage. This process

led to having two values (that of the first attempt and a conservative one) for constituting a range for the mean damage grade. This approach was revealed to have a better fitting with the field observations since 93.41% of the predicted and real/observed defined intervals are overlapped.

A third approach was performed by the means of Machine Learning techniques, specifically by using a Random Forest Classification algorithm. This algorithm was trained for solving the categorization of the level of damage by establishing other relations among the parameters rather than the one used for the analytical approach. Despite the overall performance of the model, it is considered satisfactory (with an accuracy score of 94.12%), since these results are limited to the size and typology of the sample. The analysis of the proportional importance of the parameters demonstrates that the trained model would not be suitable for assessing constructions with a very different typology. Furthermore, the number of samples, specifically in what concerns the relatively small number of samples for the extremes of the levels of damage (no damage at all or total collapse, corresponding to $D_k = 0$ and $D_k = 5$ respectively) difficult to have a good representation of these constructions. Since the normal Gaussian distribution of damage throughout the sample cannot be statistically sustained, some approaches for generating synthetic data are not suitable. Therefore, the size of the

Table 10. Hyperparameter setup for training the RFC algorithm.

Hyperparameter	Description	Value
max_depth	The longest path between the root node and the leaf node	"None" (unlimited)
min_sample_split	The minimum number of observations in any node to split it.	Default (2)
max_leaf_nodes	Limits the growth of the tree.	"None" (unlimited)
min_samples_leaf	Minimum of samples present after splitting a node.	Default (1)
n_estimators	Number of trees in the forest.	128
max_features	Maximum number of features provided to each tree	"Auto"
bootstrap	Data point sampling method. When set as "true", there is a replacement.	True
criterion	The method used for measuring the quality of a split.	Gini

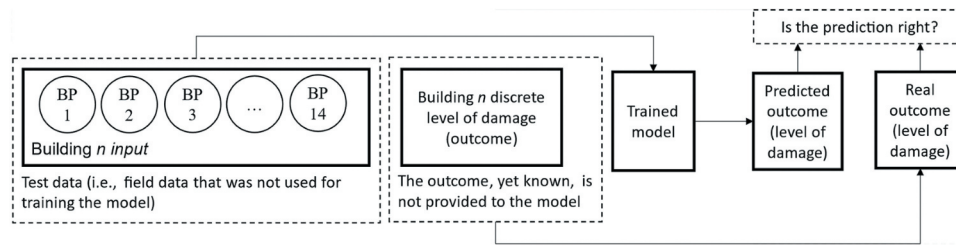


Figure 16. Schematization of the evaluation of the model.

Table 11. Classification report.

Class (D_K)	Precision	Recall	F1 score	Samples
0	1	1	1	3
1	1	1	1	8
2	1	1	1	4
3	0.92	1	0.96	12
4	0.83	0.83	0.83	6
5	0	0	0	1
Macro average	0.79	0.81	0.80	34
Weighted average	0.91	0.94	0.93	34

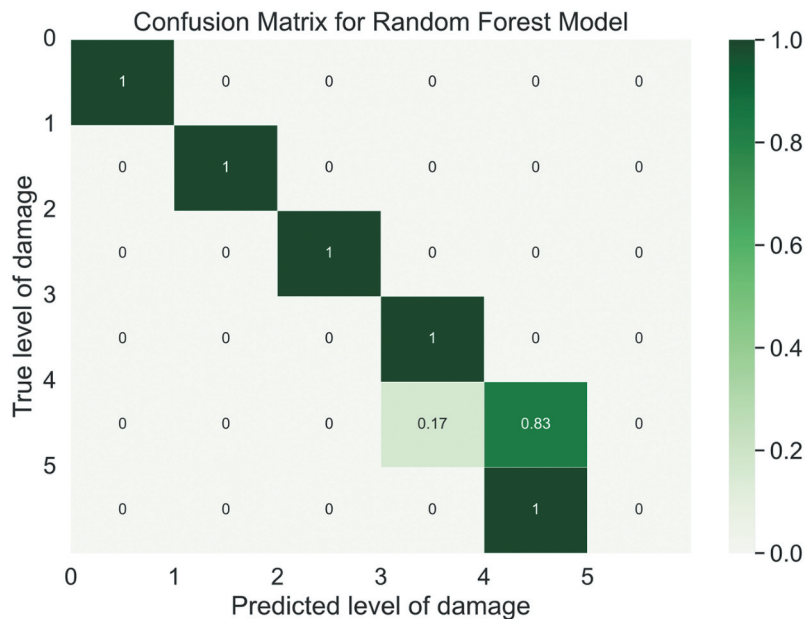


Figure 17. Confusion matrix. True values correspond to observed levels of damage.

sample is considered a limitation for obtaining more conclusions than the ones presented in this work. A necessary further development in this sense is the creation of larger datasets (based on precedent seismic events) that can be used for finding typical statistical distributions as well.

The assumption of using this algorithm as a suitable tool for similar problems is sustained given the positive results

of classifying the buildings into five damage classes. The evidence of typological fitting of the model is consistent with some empirical observations on site and offers an interesting field for enhancing the capabilities of the VIM approach by adjusting the relative weight of the parameters for diverse typologies in which there are enough data for training the model. In other words, it is possible to take advantage of the vulnerability survey as a Handcrafted

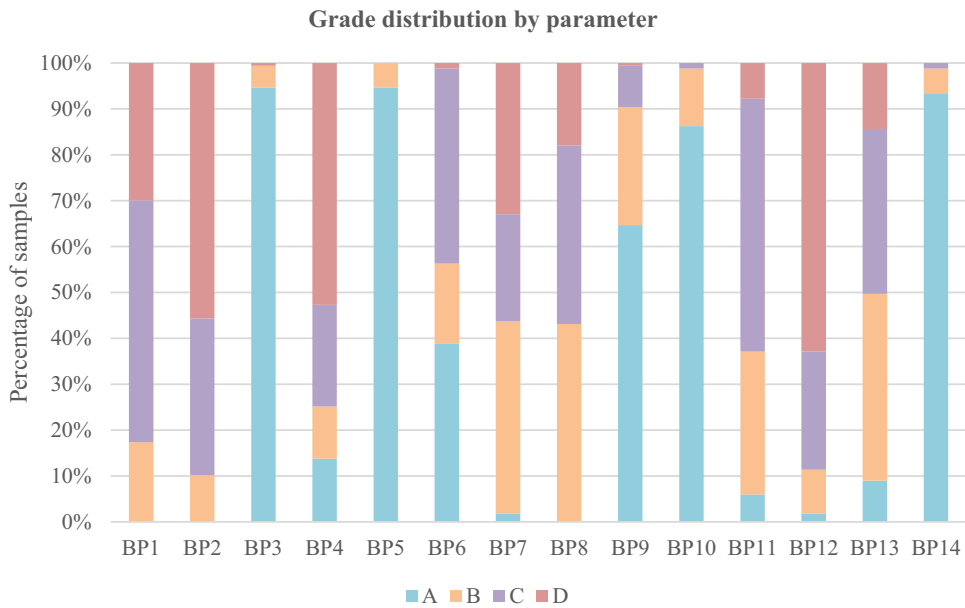


Figure 18. Vulnerability class distribution per parameter.

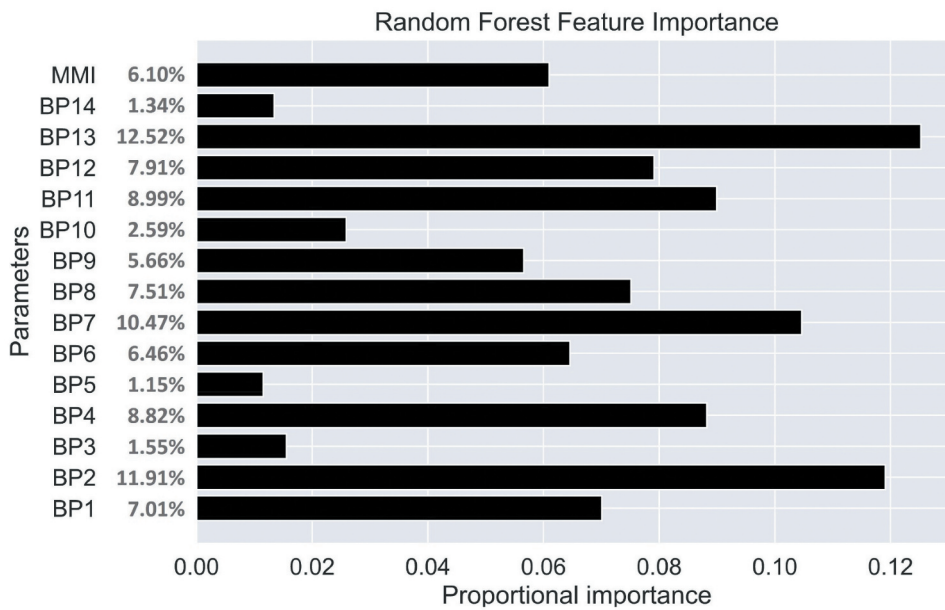


Figure 19. Relative importance by feature according to the RFC model.

Feature Extraction base for developing straightforward models under the basis of regional and/or typological sets.

The implementation process presented and discussed in this article prove that the weights originally assigned to the VIM parameters can be adjusted to obtain a better fit (for better representing) to the common vernacular typology found in Morelos. Based on this observation, it is thus possible to affirm that this same process can be applied to

develop customized models for locally built environments. The existence of information regarding previous seismic events (characterization of the constructions, levels of damage, etc.) can be used to train this ML algorithm and predict the effects that future seismic events may have on specific buildings typologies.

The tools developed for this experimental program (namely those related to data acquisition and management)

make possible the systematization and analysis of existing and new data within the workflow herein presented.

Disclosure statement

No potential conflict of interest was reported by the authors.

Funding

This work was partly financed by FCT/MCTES through national funds (PIDDAC) under the R&D Unit Institute for Sustainability and Innovation in Structural Engineering (ISISE), under reference UIDB/04029/2020. This research was funded by the Portuguese Foundation for Science and Technology (FCT) through grant number PD/BD/150385/2019. The field campaigns in the State of Morelos were financed by the Instituto de Ingeniería – Universidad Nacional Autónoma de México (Institute of Engineering – National Autonomous University of Mexico) through the project R562.

ORCID

Rafael Ramírez Eudave  <http://orcid.org/0000-0003-0733-6685>

Tiago Miguel Ferreira  <http://orcid.org/0000-0001-6454-7927>

Romeu Vicente  <http://orcid.org/0000-0002-5456-1642>

Paulo B. Lourenco  <http://orcid.org/0000-0001-8459-0199>

Fernando Peña  <http://orcid.org/0000-0002-0385-2941>

References

- Alberto, Y., M. Otsubo, H. Kyokawa, T. Kiyota, and I. Towhata. 2018. Reconnaissance of the 2017 Puebla, Mexico earthquake. *Soils and Foundations* 58 (5):1073–92. doi:10.1016/j.sandf.2018.06.007.
- Alvarado, R., and C. C. 2015. Conservación del patrimonio cultural en el Pueblo Mágico de Tepoztlán, Morelos (2001–2012). *Territorios* 16 (32):15–33. doi:10.12804/territ32.2015.01.
- Buendía, L., and E. Reinoso. 2019. Análisis DE los DAÑOS en viviendas Y edificios comerciales durante LA ocurrencia del sismo del 19 DE septiembre DE 2017. *Revista de Ingeniería Sísmica* 101 (101):19–35. doi:10.18867/ris.101.508.
- Buitinck, L., G. Louppe, M. Blondel, F. Pedregosa, A. Mueller, O. Grisel, V. Niculae, P. Prettenhofer, A. Gramfort, J. Grobler, et al. 2013. *API design for machine learning software: Experiences from the scikit-learn project* 1–15.
- Caprano, S., S. Ortiz, and R. Valencia. 2018. Los efectos económicos de los sismos de septiembre. *Revista Economía Informa* 408 (Enero–febrero):16–33.
- Centre Européen de Géodynamique et de Séismologie 1998. European macroseismic scale 1998. *Cahiers Du Centre Européen de Géodynamique et de Séismologie* 15: 99. doi:10.2312/EMS-98.full.en.
- Dash, T., S. Chitlangia, A. Ahuja, and A. Srinivasan. 2022. A review of some techniques for inclusion of domain-knowledge into deep neural networks. *Scientific Reports* 12 (1):1040. doi:10.1038/s41598-021-04590-0.
- de la Republica, S. 2017. Extensión territorial de la tragedia. *Notas Estrategicas* 1 (17):1–8.
- Dobias, M., M. Sab Varga, and P. Petrik. 2021. *Lutraconsulting/Mergin: 2021.6.1*. Zenodo. doi:10.5281/zenodo.6376045.
- Ferreira, T. M., R. Maio, and R. Vicente. 2017. Analysis of the impact of large scale seismic retrofitting strategies through the application of a vulnerability-based approach on traditional masonry buildings. *Earthquake Engineering and Engineering Vibration* 16 (2):329–48. doi:10.1007/s11803-017-0385-x.
- Galvis, F., E. Miranda, P. Heresi, H. Davalos, and J. R. Silos. 2017. Preliminary statistics of collapsed buildings in Mexico city in the september 19, 2017 puebla-morelos earthquake. John A. Blume Earthquake Engineering Center, Stanford University (Issue October).
- Geodetic Facility for the Advancement of Geoscience. (2023). *September 19, 2017 M7.1 Earthquake 5km ENE of Raboso, Mexico Data Event Response*. 2017 UNAVCO Highlights. <https://www.unavco.org/highlights/2017/2017.html>
- GNDT. 1993. *Manuale Per Il Rilevamento Della Vulnerabilità Sísmica Degli Edifici*.
- Gobierno del Distrito Federal. 2017. Decreto por el que se reforman y adicionan diversas disposiciones del Reglamento de Construcciones del Distrito Federal. *Gaceta Oficial de La Ciudad de México* 188: 2–701.
- Godínez, E., A. Tena, H. Archundia, A. Gómez, R. Ruíz, and J. Escamilla. 2019. Structural damage in housing and apartment buildings located in the Southeast of Mexico due to the september sismo de tehuantepec del 7 de septiembre. *Revista Internacional de Ingeniería de Estructuras* 24 (2):223–58.
- Guerrero Baca, L. F. 2019. Comportamiento sísmico de viviendas tradicionales de adobe, situadas en las faldas del volcán Popocatepetl, México. *Gremium* 6 (11):104–17. doi:10.56039/rgn11a11.
- Guyon, I., and A. Elisseeff. 2006. An introduction to feature extraction. *Studies in Fuzziness and Soft Computing* 207:1–25. doi:10.1007/978-3-540-35488-8_1.
- Han, J., J. Kim, S. Park, S. Son, and M. Ryu. 2020. Seismic vulnerability assessment and mapping of gyeongju, South Korea using frequency ratio, decision tree, and random forest. *Sustainability* 12 (18):7787. doi:10.3390/su12187787.
- INAH. 2019. *Catálogo Nacional de Monumentos Históricos Inmuebles*. Centro de Documentación de La CNMH. <https://catalogonacionalmhi.inah.gob.mx/consultaPublica>.
- INEGI - Instituto Nacional de Estadística y Geografía *Encuesta Intercensal 2015. Subsistema de Información Demográfica y Social*. 2023. <https://www.inegi.org.mx/programas/intercensal/2015/#Microdatos>.
- Khurana, U., H. Samulowitz, and D. Turaga. 2018. Feature engineering for predictive modeling using reinforcement learning. *Proceedings of the AAAI Conference on Artificial Intelligence* 32 (1). doi:10.1609/aaai.v32i1.11678.
- Lei, X., L. Sun, Y. Xia, and T. He. 2020. Vibration-based seismic damage states evaluation for regional concrete beam bridges using random forest method. *Sustainability* 12 (12):5106. doi:10.3390/su12125106.

- Midwinter, M., C. M. Yeum, and E. Kim. 2022. *Explainable machine learning for seismic vulnerability assessment of low-rise reinforced concrete buildings* 371–79. doi: [10.1007/978-981-19-0656-5_31](https://doi.org/10.1007/978-981-19-0656-5_31).
- Mishra, M. 2021. Machine learning techniques for structural health monitoring of heritage buildings: A state-of-the-art review and case studies. *Journal of Cultural Heritage* 47:227–45. doi: [10.1016/j.culher.2020.09.005](https://doi.org/10.1016/j.culher.2020.09.005).
- Ortiz, R. M., R. F. Reséndiz, C. M. J. Ortiz, R. M. Martínez, C. M. Ortiz, and C. A. G. Bazán. 2018. El sismo del 19 de septiembre. ¿Cómo enfrentamos la crisis en Morelos, México? *Cadernos Metrópole* 20 (42):325–45. doi: [10.1590/2236-9996.2018-4202](https://doi.org/10.1590/2236-9996.2018-4202).
- Oshiro, T. M., P. S. Perez, and J. A. Baranauskas. 2012. *How many trees in a random forest?* 154–68. doi: [10.1007/978-3-642-31537-4_13](https://doi.org/10.1007/978-3-642-31537-4_13).
- Pedregosa, F., G. Varoquaux, A. Gramfort, V. Michel, B. Thirion, O. Grisel, M. Blondel, A. Müller, J. Nothman, G. Louppe, et al. 2012. Scikit-learn: Machine Learning in Python. *Journal of Machine Learning Research* 12:2825–30.
- Peppoloni, S., and G. Di Capua. 2021. Current definition and vision of geoethics. In *Geo-societal Narratives*, 17–28. Springer International Publishing. doi: [10.1007/978-3-030-79028-8_2](https://doi.org/10.1007/978-3-030-79028-8_2).
- QGIS Development Team. (2021). *QGIS Geographic Information System*. <https://www.qgis.org>
- Quintana Leonardo, M., and S. L. F. Guerrero Baca Luis. 2010. La casa tradicional de adobe en Yecapixtla, México: Un análisis tipológico. *Arquitectura Construida En Tierra, Tradición e Innovación. Congresos de Arquitectura de Tierra En Cuenca de Campos 2004/2009*:155–66.
- Ramírez Eudave, R. 2022. Seismic vulnerability calculator and database (software). 2.0. doi: [10.5281/zenodo.7180849](https://doi.org/10.5281/zenodo.7180849).
- Ramírez Eudave, R., and T. M. Ferreira. 2021. On the potential of using the Mexican national catalogue of historical monuments for assessing the seismic vulnerability of existing buildings: A proof-of-concept study. *Bulletin of Earthquake Engineering* 19 (12):4945–78. doi: [10.1007/s10518-021-01154-5](https://doi.org/10.1007/s10518-021-01154-5).
- Ramírez Eudave, R., T. M. Ferreira, and R. Vicente. 2022. Parameter-based seismic vulnerability assessment of Mexican historical buildings: Insights, suitability, and uncertainty treatment. *International Journal of Disaster Risk Reduction* 74:102909. doi: [10.1016/j.ijdr.2022.102909](https://doi.org/10.1016/j.ijdr.2022.102909).
- Ramírez Eudave, R., D. Rodrigues, T. M. Ferreira, and R. Vicente. 2023. Implementing Open-Source Information Systems for Assessing and Managing the Seismic Vulnerability of Historical Constructions. *Buildings, MDPI* 13 (2):540. doi: [10.3390/buildings13020540](https://doi.org/10.3390/buildings13020540).
- Rosti, A., M. Rota, and A. Penna. 2021. Empirical fragility curves for Italian URM buildings. *Bulletin of Earthquake Engineering* 19 (8):3057–76. doi: [10.1007/s10518-020-00845-9](https://doi.org/10.1007/s10518-020-00845-9).
- Ruggieri, S., M. Calò, A. Cardellicchio, and G. Uva. 2022. Analytical-mechanical based framework for seismic overall fragility analysis of existing RC buildings in town compartments. *Bulletin of Earthquake Engineering* 20 (15):8179–216. doi: [10.1007/s10518-022-01516-7](https://doi.org/10.1007/s10518-022-01516-7).
- Ruggieri, S., A. Cardellicchio, V. Leggieri, and G. Uva. 2021. Machine-learning based vulnerability analysis of existing buildings. *Automation in Construction* 132:103936. doi: [10.1016/j.autcon.2021.103936](https://doi.org/10.1016/j.autcon.2021.103936).
- Sahakian, V. J., D. Melgar, L. Quintanar, L. Ramírez-guzmán, X. Pérez-campos, and A. Baltay. 2018. Ground motions from the 7 and 19 September 2017 Tehuantepec and Puebla-Morelos, Mexico, Earthquakes. *Bulletin of the Seismological Society of America* 108 (6):3300–12. doi: [10.1785/0120180108](https://doi.org/10.1785/0120180108).
- Salazar, L. G., and T. M. Ferreira. 2020. Seismic vulnerability assessment of historic constructions in the downtown of Mexico City. *Sustainability* 12 (3):1276. doi: [10.3390/su12031276](https://doi.org/10.3390/su12031276).
- Sánchez Calvillo, A., E. M. Alonso Guzmán, and M. D. C. López Núñez. 2021. Vulnerabilidad sísmica y la pérdida de la vivienda de adobe en Jojutla, Morelos, México, tras los sismos de 2017. *Vivienda y Comunidades Sustentables* 10 (10):9–29. doi: [10.32870/rvcs.v2i10.162](https://doi.org/10.32870/rvcs.v2i10.162).
- UNESCO. (2016). *The HUL Guidebook: Managing heritage in dynamic and constantly changing urban environments. The 15th World Conference of the League of Historical Cities*, 59. <http://historicurbanlandscape.com/themes/196/userfiles/download/2016/6/7/wirey5prpznidqx.pdf>
- UNISDR - United Nations Office for Disaster Risk Reduction. (2017). *GAR Atlas: Unveiling Global Disaster Risk* (UNISDR - United Nations Office for Disaster Risk Reduction (ed.); 1st ed.). Imprimerie Gonnet. https://www.preventionweb.net/files/53086_garatlasr2.pdf
- United Nation. (2015). General Assembly: resolution adopted by the general assembly on 3 june 2015. *2015 Third UN World Conference on Disaster Risk Reduction (WCDRR)*, 08955(June), 1–24.
- United Nations International Strategy for Disaster Risk Reduction. 2009. Terminology on disaster risk reduction. doi: [10.7591/9781501701498-008](https://doi.org/10.7591/9781501701498-008).
- USGS. (2017). *M 7.1 - 1km E of Ayutla, Mexico*. (Last revised: February/2020). Earthquake Hazards Program. <https://earthquake.usgs.gov/earthquakes/eventpage/us2000ar20/map?historic-seismicity=true&shakemap-intensity=false>
- Vadyala, S. R., S. N. Betgeri, J. C. Matthews, and E. Matthews. 2022. A review of physics-based machine learning in civil engineering. *Results in Engineering* 13:100316. doi: [10.1016/j.rineng.2021.100316](https://doi.org/10.1016/j.rineng.2021.100316).
- Zatarain, K. (2017). *Peña Nieto afirma erróneamente que “la caída de viviendas [tras el sismo en Oaxaca] se debió a que están hechas de adobe.”* ArchDaily México. <https://www.archdaily.mx/mx/880216/pena-nieto-afirma-erroneamente-que-la-caida-de-viviendas-tras-el-sismo-en-oaxaca-se-debio-a-que-estan-hechas-de-adobe>